

Cross-Section Calculations on Several Structural Fusion Materials for $(\gamma,3n)$ Reactions in the Photon Energy Range of 20–110 MeV

A. Kaplan · V. Çapalı

Published online: 29 January 2014
© Springer Science+Business Media New York 2014

Abstract In this study, photo-neutron cross-sections of $(\gamma,3n)$ reactions for several structural fusion materials such as ^{55}Mn , ^{65}Cu , ^{94}Zr , $^{98,100}\text{Mo}$, ^{181}Ta and ^{186}W have been investigated in the incident photon energy range of 20–110 MeV. Theoretical cross-section calculations, based on theoretical nuclear reaction models, have been carried out using the PCROSS, EMPIRE 3.1 and TALYS 1.6 codes. EMPIRE 3.1 exciton, TALYS 1.6 two component exciton and TALYS 1.6 pre-equilibrium models have been used to calculate the pre-equilibrium photo-neutron cross-sections. For the equilibrium cross-section calculations, PCROSS Weisskopf–Ewing model has been preferred. The calculated results have been compared with each other and against the experimental nuclear reaction data (EXFOR). Except the $^{65}\text{Cu}(\gamma,3n)^{62}\text{Cu}$ reaction, all model equilibrium and pre-equilibrium cross-section calculations exhibit generally good agreement with the experimental values for all reactions used in this study. TALYS 1.6 two component exciton model can be recommended, if experimental photo-neutron cross-section data are not available or are unlikely to be produced because of the experimental difficulties.

Keywords Photo-neutron cross-section · $(\gamma,3n)$ Reaction · Structural fusion materials · EXFOR database

Introduction

Current research and development activities on materials for fusion power reactors are mainly focused on plasma facing, tritium breeding and structural materials [1]. The current approach to developing structural materials for fusion reactors requires a heavy reliance on the use of small irradiation specimens largely because of limitations in available irradiation volumes [2]. The selection of fusion structural materials are an indispensable component for fusion reactor technology [3]. Intense neutron fluxes within fusion reactors that are currently being designed will lead to the activation of structural components. To evaluate and reduce this radiation, nuclear cross-section data are required for neutrons [4].

The reaction cross-section data have a critical importance on fusion reactors and development for fusion reactor technology. In a fusion reactor design, neutron reaction cross-section data are required and the evaluated values in nuclear data files are usually used for neutronic calculations [5–7]. Besides, photonuclear cross-sections are also important for some applications as; analysis of radiation transport and shielding, absorbed dose calculations in the human body throughout photon-radiotherapy, fission and fusion reactor technology, activation analysis including protections and material analysis studies for photon-induced reactions and transmutation of nuclear waste [8, 9].

The nuclear reaction models are generally required to get the prediction of the reaction cross-sections, especially if the no experimental data obtained or in cases where it is difficult to carry out the experimental measurements [10–15].

In our previous studies [7, 12], we examined (γ,n) and $(\gamma,2n)$ photo-neutron cross-sections of several structural

A. Kaplan (✉) · V. Çapalı
Department of Physics, Faculty of Arts and Sciences, Süleyman Demirel University, Isparta, Turkey
e-mail: abdullahkaplan@sdu.edu.tr

fusion materials. In this study, the theoretical ($\gamma,3n$) reaction cross-sections of several structural fusion materials such as ^{55}Mn , ^{65}Cu , ^{94}Zr , $^{98,100}\text{Mo}$, ^{181}Ta and ^{186}W in photon-induced reactions have been investigated. The photo-neutron cross-sections of $^{55}\text{Mn}(\gamma,3n)^{52}\text{Mn}$, $^{65}\text{Cu}(\gamma,3n)^{62}\text{Cu}$, $^{94}\text{Zr}(\gamma,3n)^{91}\text{Zr}$, $^{98}\text{Mo}(\gamma,3n)^{95}\text{Mo}$, $^{100}\text{Mo}(\gamma,3n)^{97}\text{Mo}$, $^{181}\text{Ta}(\gamma,3n)^{178}\text{Ta}$ and $^{186}\text{W}(\gamma,3n)^{183}\text{W}$ reactions have been calculated using PCROSS [16], EMPIRE 3.1 [17, 18] and TALYS 1.6 [19] computer codes in the photon energy range of 20–110 MeV. EMPIRE 3.1 exciton, TALYS 1.6 two component exciton and TALYS 1.6 pre-equilibrium models have been used to calculate the pre-equilibrium photo-neutron cross-sections. PCROSS Weisskopf–Ewing (WE) [20] model have been used for the reaction equilibrium component. The calculated results have been compared with each other and available experimental data existing in the EXFOR [21] database.

Calculation Methods

Photo-neutron cross-sections as a function of photon energy have been calculated using PCROSS code for the WE model, EMPIRE 3.1 code for the exciton model and TALYS 1.6 code for the two component exciton and pre-equilibrium models.

The equilibrium particle emission is given by the WE model in which angular momentum conservation is neglected. In the process, the basic parameters are inverse reaction cross-section, binding energies, the pairing and the level density parameters. The reaction cross-section for incident channel a and exit channel b can be written as

$$\sigma_{ab}^{WE} = \sigma_{ab}(E_{inc}) \frac{\Gamma_b}{\sum_{b'} \Gamma_{b'}} \tag{1}$$

where E_{inc} is the incident energy. In Eq. (1), Γ_b can be also expressed as

$$\Gamma_b = \frac{2s_b + 1}{\pi^2 \hbar^2} \mu_b \int d\varepsilon \sigma_b^{inv}(\varepsilon) \varepsilon \frac{\omega_1(U)}{\omega_1(E)} \tag{2}$$

where U , μ_b , s_b are the excitation energy of the residual nucleus, the reduced mass and the spin, respectively. The total single-particle level density is taken as

$$\omega_1(E) = \frac{1}{\sqrt{48}} \frac{\exp[2\sqrt{\alpha(E-D)}]}{E-D}; \alpha = \frac{6}{\pi^2} g \tag{3}$$

where σ_b^{inv} , E , D and g are the inverse reaction cross-section, the excitation energy of the compound nucleus, the pairing energy and the single-particle level density, respectively.

The EMPIRE 3.1 includes the pre-equilibrium mechanism as defined in the exciton model [22], as based on the

solution of the master equation [23] in the form proposed by Cline [24] and Ribansky [25]

$$-q_{t=0}(n) = \lambda_+(E, n+2)\tau(n+2) + \lambda_-(E, n-2)\tau(n-2) - [\lambda_+(E, n) + \lambda_-(E, n) + L(E, n)]\tau(n) \tag{4}$$

where $q_t(n)$ is the initial occupation probability of the composite nucleus in the state with the exciton number n , $\lambda_+(E, n)$ and $\lambda_-(E, n)$ are the transition rates for decay to neighboring states, and $L(E, n)$ is the total emission rate integrated over emission energy for particles (protons π , neutrons ν and clusters) and γ -rays.

The pre-equilibrium spectra can be calculated as

$$\frac{d\sigma_{a,b}}{d\varepsilon_b}(\varepsilon_b) = \sigma_{a,b}^r(E_{inc}) D_{a,b}(E_{inc}) \times \sum_n W_b(E, n, \varepsilon_b) \tau(n) \tag{5}$$

where $\sigma_{a,b}^r(E_{inc})$ is the cross-section of the reaction (a, b), $W_b(E, n, \varepsilon_b)$ is the probability of emission of a particle of type b (or γ ray) with energy ε_b from a state with n excitons and excitation energy E of the compound nucleus, and $D_{a,b}(E_{inc})$ is the depletion factor, which takes into account the flux loss as a result of the direct reaction processes.

TALYS [19, 26] is a nuclear reaction simulation code for the estimation and analysis of nuclear reactions that include protons, neutrons, photons, tritons, deuterons, ^3He and alpha particles in the energy range of 1 keV–200 MeV. For this, TALYS integrates the optical model, direct, pre-equilibrium, fission and statistical nuclear reaction models in one calculation scheme and thereby gives a prediction for all the open reaction channels. In TALYS, several options are included for the choice of different parameters such as γ -strength functions, nuclear level densities and nuclear model parameters [27]. The pre-equilibrium reactions were considered by the two component exciton model [28]. The pre-equilibrium model of TALYS is the two-component exciton model of Kalbach [29]. In the two component model, the neutron and proton type of the created particles and holes is explicitly followed throughout the reaction.

The details of the other code model parameters and options of TALYS can be found in Refs. [19, 26].

Results and Discussion

In the present study, ($\gamma,3n$) reaction cross-sections of $^{55}\text{Mn}(\gamma,3n)^{52}\text{Mn}$, $^{65}\text{Cu}(\gamma,3n)^{62}\text{Cu}$, $^{94}\text{Zr}(\gamma,3n)^{91}\text{Zr}$, $^{98}\text{Mo}(\gamma,3n)^{95}\text{Mo}$, $^{100}\text{Mo}(\gamma,3n)^{97}\text{Mo}$, $^{181}\text{Ta}(\gamma,3n)^{178}\text{Ta}$ and $^{186}\text{W}(\gamma,3n)^{183}\text{W}$ reactions have been performed in the photon energy range of 20–110 MeV using PCROSS, EMPIRE 3.1 and TALYS 1.6 computer codes. The photo-

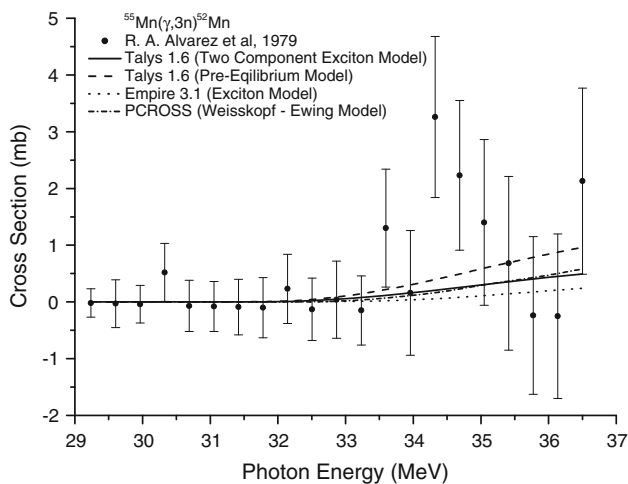


Fig. 1 Calculated values for the $^{55}\text{Mn}(\gamma,3n)^{52}\text{Mn}$ reaction with experimental data taken from EXFOR

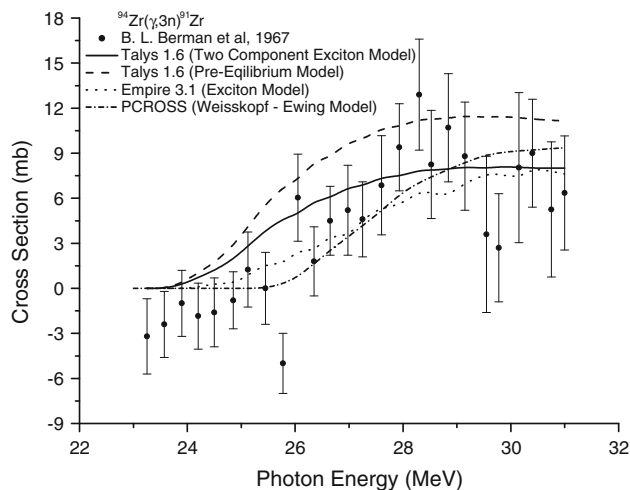


Fig. 3 The same as Fig. 1 but for $^{94}\text{Zr}(\gamma,3n)^{91}\text{Zr}$

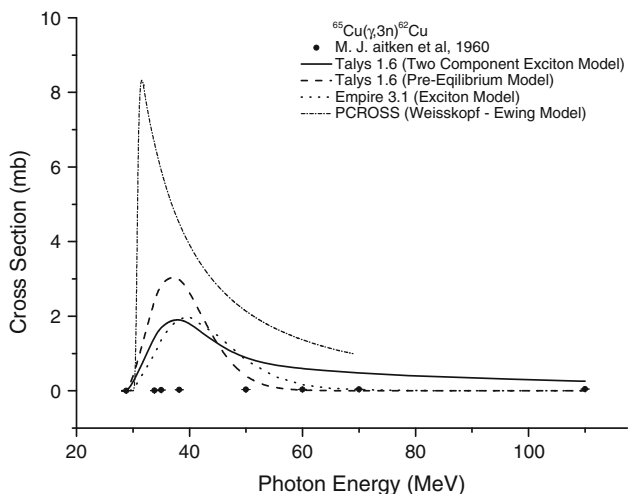


Fig. 2 The same as Fig. 1 but for $^{65}\text{Cu}(\gamma,3n)^{62}\text{Cu}$

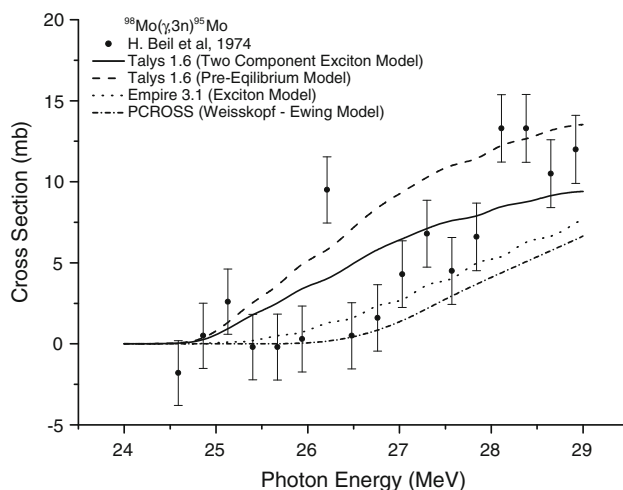


Fig. 4 The same as Fig. 1 but for $^{98}\text{Mo}(\gamma,3n)^{95}\text{Mo}$

neutron cross-sections shown by $(\gamma,3n)$ reactions for ^{55}Mn , ^{65}Cu , ^{94}Zr , $^{98,100}\text{Mo}$, ^{181}Ta and ^{186}W target nuclei have been plotted as a function of photon energy in Figs. 1, 2, 3, 4, 5, 6 and 7. All experimental values used in this study have been taken from the EXFOR database. In the EXFOR library, the experimental cross-section data concerning $(\gamma,3n)$ reactions are scarce for the structural fusion materials worked in this study.

The calculated photo-neutron cross-sections of $^{55}\text{Mn}(\gamma,3n)^{52}\text{Mn}$ reaction have been compared with the experimental values in Fig. 1. All theoretical model calculations are in good agreement with the experimental data in the photon energy region 29–32.5 MeV. Although PCROSS, EMPIRE 3.1 and TALYS 1.6 model calculations

exhibit a little discrepancy with each other in the photon energy region 32.5–36.5 MeV, in general, they are in agreement with the experimental data including error bars. $^{65}\text{Cu}(\gamma,3n)^{62}\text{Cu}$ reaction cross-section calculations have been compared with the experimental data in Fig. 2. The PCROSS-WE calculations are not in good agreement with the experimental values. The PCROSS code can work legally up to 69 MeV incident photon energy. Therefore, the PCROSS-WE calculations have been shown up to 69 MeV. EMPIRE 3.1 exciton, TALYS 1.6 two component exciton and pre-equilibrium model calculations are in harmony with each other. The TALYS 1.6 pre-equilibrium curves fit the experimental values the best in the energy range of 60–110 MeV. The theoretical model calculations of $^{94}\text{Zr}(\gamma,3n)^{91}\text{Zr}$ reaction have been compared with the

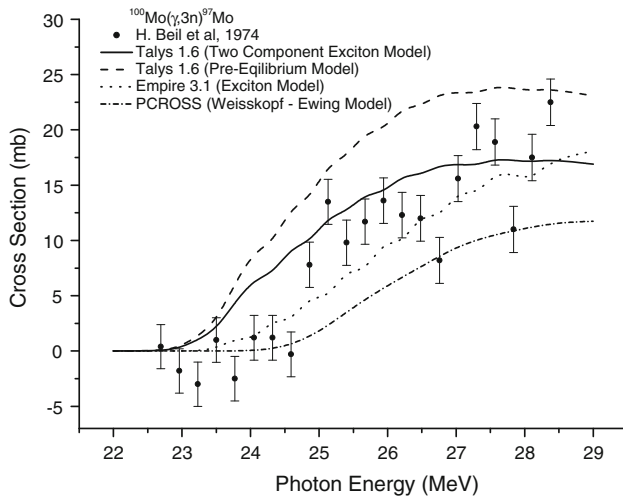


Fig. 5 The same as Fig. 1 but for $^{100}\text{Mo}(\gamma,3n)^{97}\text{Mo}$

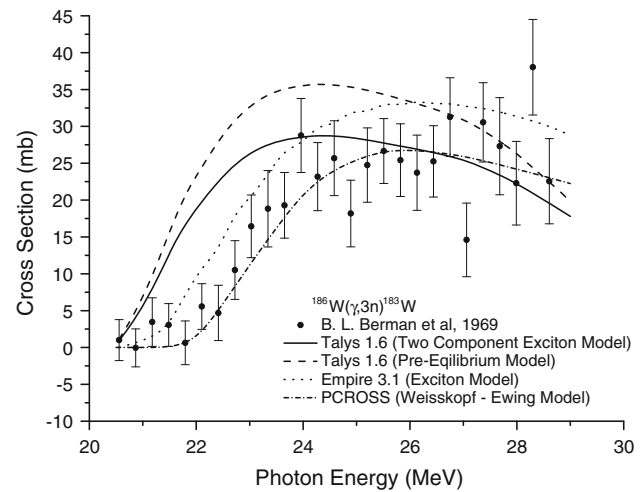


Fig. 7 The same as Fig. 1 but for $^{186}\text{W}(\gamma,3n)^{183}\text{W}$

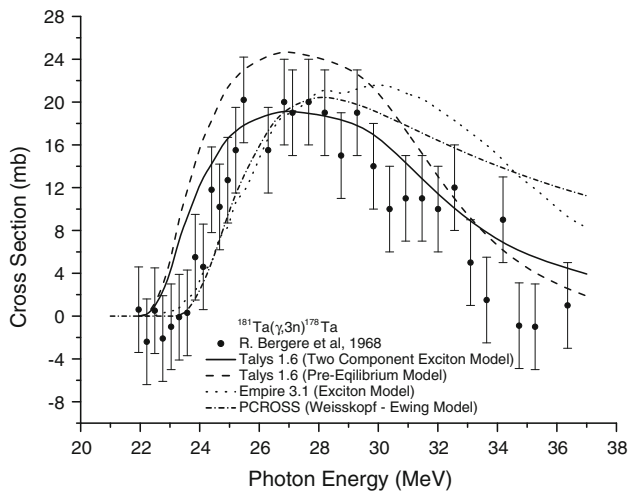


Fig. 6 The same as Fig. 1 but for $^{181}\text{Ta}(\gamma,3n)^{178}\text{Ta}$

experimental results in Fig. 3. All photo-neutron cross-sections are in agreement with the experimental values including error bars in the photon energy region 24–31 MeV. The calculated values of $(\gamma,3n)$ reactions for $^{98,100}\text{Mo}$ target nuclei have been compared with the experimental data in Figs. 4, 5. All theoretical model calculations are in agreement with the experimental data including error bars at the photon energy regions 24.5–29 MeV for the $^{98}\text{Mo}(\gamma,3n)^{95}\text{Mo}$ and 22.5–28.5 MeV for the $^{100}\text{Mo}(\gamma,3n)^{97}\text{Mo}$ reactions. The TALYS 1.6 pre-equilibrium model calculations are higher than the other theoretical calculations and experimental values in Fig. 5. The TALYS 1.6 two component exciton model cross-sections are shown to have a good agreement with the

experimental data. The comparison of theoretical and experimental results of $^{181}\text{Ta}(\gamma,3n)^{178}\text{Ta}$ reaction has been given in Fig. 6. PCROSS-WE and EMPIRE 3.1 model calculations are in agreement with the measurements in the 22–28 MeV photon energy region. The TALYS 1.6 pre-equilibrium model calculations follow the experimental results from above up to 32 MeV but the TALYS 1.6 two component exciton model cross-sections are the best agreement with the measurements including error bars. The theoretical cross-section calculations and experimental values of $^{186}\text{W}(\gamma,3n)^{183}\text{W}$ reaction have been given in Fig. 7. Generally the PCROSS-WE and EMPIRE 3.1 model calculations are in harmony with the measurements in the energy region of 20–29 MeV. The PCROSS-WE model results are in good agreement with the experimental data. The TALYS 1.6 two component exciton model cross-sections are in agreement with the experimental data in the 24–28 MeV but the TALYS 1.6 pre-equilibrium model results are the best agreement with the experimental values in the 26.5–29 MeV photon energy region.

In general Figs. 1, 2, 3, 4, 5, 6 and 7 show that PCROSS, EMPIRE 3.1 and TALYS 1.6 model calculations exhibit a similar structure with experimental data except for $^{65}\text{Cu}(\gamma,3n)^{62}\text{Cu}$ reaction. As we can see from these results, the good agreement between photo-neutron cross-section calculations and experimental values of $(\gamma,3n)$ reactions shows that PCROSS, EMPIRE 3.1 and TALYS 1.6 models are able to reproduce the cross-sections with reasonable accuracy in this case even without any tuning of the parameters. Besides, the agreement with the theoretical values obtained with TALYS 1.6 using two component exciton model parameters proves again the prediction strength of the code.

Summary and Conclusions

In this study, theoretical photo-neutron cross-sections of ($\gamma,3n$) reactions for several structural fusion materials such as ^{55}Mn , ^{65}Cu , ^{94}Zr , $^{98,100}\text{Mo}$, ^{181}Ta and ^{186}W have calculated in the photon energy range of 20–110 MeV using PCROSS, EMPIRE 3.1 and TALYS 1.6 computer codes. The calculated results have been also compared with the available experimental values in the EXFOR library. The results can be summarized and concluded as follows:

1. The photo-neutron cross-section results calculated with PCROSS, EMPIRE 3.1 and TALYS 1.6 computer codes for ($\gamma,3n$) reaction are mostly in agreement with the experimental data except for $^{65}\text{Cu}(\gamma,3n)^{62}\text{Cu}$ reaction.
2. All model cross-section calculations are in good harmony with each other for all reactions in this study.
3. The good agreement between the calculations and experimental values shows that PCROSS, EMPIRE 3.1 and TALYS 1.6 models are able to reproduce the cross-sections with reasonable accuracy in this case even without any tuning of the parameters.
4. The agreement with the theoretical results obtained with TALYS 1.6 using two component exciton model parameters proves again the prediction strength of the code.
5. The TALYS 1.6 two component exciton option for ($\gamma,3n$) reaction cross-section calculations can be chosen, if the experimental data are not available or are improbable to be produced due to the experimental difficulty.

Acknowledgments This work has been supported by the Süleyman Demirel University Scientific Research Projects Coordination Unit (Project No: 3748-D2-13).

References

1. N. Baluc et al., Nucl. Fusion **47**, S696 (2007)
2. G.E. Lucas et al., Trans. Am. Nucl. Soc. (United States) **52**; Conference: American Nuclear Society Annual Meeting. Reno, NV, USA, 15 Jun 1986 (1986)
3. M. Yiğit et al., J. Fusion Energy. **32**, 317 (2013)
4. M.B. Chadwick et al., Fusion Eng. Des. **37**(1), 79 (1997)
5. H. Aytekin et al., J. Fusion Energy. **30**, 21 (2011)
6. T. Nishio et al., J. Nucl. Sci. Technol. **2**, 955 (2002)
7. A. Kaplan et al., J. Fusion Energy. **32**, 344 (2013)
8. M.B. Chadwick et al., in *Handbook on Photonuclear Data for Applications Cross-sections and Spectra, Final Report of a Co-ordinated Research Project 1996–1999, IAEA-TECDOC-1178*. (International Atomic Energy Agency, Vienna, 2000)
9. B.S. Ishkhanov, V.V. Varlamov, Phys. At. Nucl. **67**, 1664 (2004)
10. E. Tel et al., J. Fusion Energy. **32**, 304 (2013)
11. A. Kaplan, J. Fusion Energy. **32**, 382 (2013)
12. A. Kaplan et al., J. Fusion Energy. **32**, 431 (2013)
13. H. Aytekin et al., J. Radioanal. Nucl. Chem. **298**, 95 (2013)
14. A. Aydın et al., J. Fusion Energy. **27**, 308 (2008)
15. E. Tel et al., J. Fusion Energy. **31**, 184 (2012)
16. R. Capote et al., Final Report on Research Contract 5472/RB, INDC(CUB)-004 (Higher Institute of Nuclear Science and Technology, Cuba), Translated by the IAEA on March 1991 (PCROSS program code)
17. M. Herman et al., Nucl. Data Sheets **108**, 2655 (2007)
18. M. Herman et al., EMPIRE-3.1 Rivoli Modular System for Nuclear Reaction Calculations and Nuclear Data Evaluation, User's Manual (2012)
19. A. Koning, S. Hilaire, S. Goriely, *TALYS-1.6 A Nuclear Reaction Program, User Manual*, 1st edn (NRG, The Netherlands, 2013)
20. V.F. Weisskopf, D.H. Ewing, Phys. Rev. **57**, 472 (1940)
21. Brookhaven National Laboratory, National Nuclear Data Center, EXFOR/CSISRS (Experimental Nuclear Reaction Data File). Database Version of November 20, 2013 (2013), (<http://www.nndc.bnl.gov/exfor/>)
22. J.J. Griffin, Phys. Rev. Lett. **17**, 478 (1966)
23. C. Cline, M. Blann, Nucl. Phys. A **172**, 225 (1971)
24. C.K. Cline, Nucl. Phys. A **193**, 417 (1972)
25. I. Ribansky et al., Nucl. Phys. A **205**, 545 (1973)
26. A.J. Koning, S. Hilaire, M.C. Duijvestijn, TALYS: comprehensive nuclear reaction modeling, in *Proceedings of the International Conference on Nuclear Data for Science and Technology-ND 2004, AIP*, ed. by R.C. Haight, M.B. Chadwick, T. Kawano, P. Talou, vol 769 (Santa Fe, 2005), pp. 1154–1159
27. R. Crasta et al., J. Radioanal. Nucl. Chem. **290**, 367 (2011)
28. A.J. Koning, M.C. Duijvestijn, Nucl. Phys. A **744**, 15 (2004)
29. C. Kalbach, Phys. Rev. C **33**, 818 (1986)